NUMERICAL SIMULATION OF ULTRA- STRENGTH CONCRETE-FILLED STEEL COLUMNS

Z. Yang [1, 2*] – Y. Zhang [1] – M. Chen [2] – G. Chen [2]

[1]College of Civil Engineering and Architecture, Central South University, Changsha 410081, Hunan, China
[2] College of Civil Engineering, Putian University, Putian 351100, Fujian, China

ARTICLE INFO	Abstract:
	Researches into the constitutive relation of the super high strength and high performance concrete and the stress strain relationship of the ultra-strength concrete-filled steel columns are rare. Therefore, this paper based on continuous mechanics presents the relationship of mathematical description to the concrete deformation behaviors. The compressive behaviors of steel-reinforced super high-strength concrete columns under axial loading were studied with a series of experiments. Two specimens with concrete strengths ranging from 130,1MPa to 137,3MPa and with 121mm circular hollow stub columns with wall thicknesses of 5 mm were manufactured. At the same time, a three dimensional non-linear FE analysis of axial compression was conducted using the finite element program ABAQUS/Standard solver. The numerical results were validated through comparison with experimental data in terms of axial loading and deformation modes.

1   Introduction

Because it is recognized that the axial load-bearing capacity of a concrete-filled steel column may be higher than the sum of the axial load-bearing capacities of the concrete core and the corresponding hollow steel section, the concrete filled steel tube structures have been widely used such as in high-rise buildings and long-span structures. The use of concrete-filled composite columns may be dated back to the 1960s [1-3]. The state of art review on steel–concrete composite columns by Shanmugam and Lakshmi [4] highlighted the significant research into this field. Most of the researchers focused on concrete-filled tubular columns with normal concrete [5-8].

With the development of economy and the depletion of resources, the concrete-filled steel column should get higher performance. So, being higher with the

specific strength and lower with the consumption of natural resource and the cost in their life cycle, reactive powder concrete as the representative of green super high strength concrete is of a promising application and has become the focus of research and application to the modern concrete. However, the structural behavior of concrete-filled tube columns is affected by many factors, such as member material properties, column slenderness and the geometry of steel section. Simultaneously, domestic and foreign researches done on super high-strength concrete composite members are rare. This necessitates the search for the compressive behavior of the super high strength concrete used in stone-chip steel tube columns.

To enable better understanding of the compressive behavior of the ultra-high strength concrete-filled steel tubular columns, the constitutive relation of the super high strength and high performance concrete

---

[*] Corresponding author. Tel.:+8615160230829; fax:+8605942676110
E-mail address: zhisyang@yeah.net.

was studied. First, the constitutive relation is derived by the vector method. Second, as an excellent method of the finite element method, it has a large number of applications in many engineering and scientific research fields [9-11]. A finite element model was developed through the ABAQUS/standard solver to predict the axial compressive resilience of the ultra-high strength concrete-filled steel tubular columns. Finally, validation of this numerical method is carried out by comparing the simulation results with the experimental observation of two physical tests carried out at Central South University. It is expected that the simulation will be used to carry out studies for this type of structure in years to come.

2   Theoretical analysis

For short concrete-filled tubular columns with circular hollow sections under compression, the stress–strain relationship of the confined concrete, etc., have been established and verified by researchers worldwide[12-17].However, the axial compressive behavior of the super high strength concrete is much less researched. This article refers to [18]. The relationship of Strain tensor components and stress tensor components is derivable from Hooke's law:

$$\varepsilon_{ij} = \frac{\sigma_{ij}}{2G} - \frac{3\upsilon}{E}\sigma_0\delta_{ij} \tag{1}$$

Where,

ε_{ij} = the strain tensor components；

σ_{ij} = the stress tensor components；

G, E and v= shear modulus, elasticity modulus and Poisson's ratio；

$\sigma_0 = \frac{1}{3}(\sigma_{11} + \sigma_{22} + \sigma_{33})$ = mean normal stress；

σ_{11}, σ_{22} and σ_{33} = principal stresses

δ_{ij} = Kronecker

From [18], strain of concrete be expressed

$$\varepsilon_{ij} = \frac{\sigma_{ij} + \sigma_{id}\delta_{ij}}{2G_s} - \frac{3\nu}{E_s}(\sigma_0 + \sigma_{id})\delta_{ij} \tag{2}$$

Where,

σ_{id} = internal Stress

$$\sigma_{id} = \frac{k}{1 + l\left(\frac{\sigma_0}{f_c}\right)^m}\left(\frac{\tau_0}{f_c}\right)^n f_c \tag{3}$$

Where,

f_c = the cylinder crushing strength of concrete;

τ_0 = normal shear stress

k, n, m and l are material parameters which are obtained from [19];

G_s, E_s and ν_s =secant shear modulus, elasticity modulus and Poisson's ratio;

$$E_s = \frac{9K_sG_s}{3K_s + G_s}; \nu_s = \frac{3K_s - 2G_s}{6K_s + 2G_s}$$

Where, K_s = Secant bulk modulus;

So the formulae are derived below

$$\frac{K_s}{K_e} = \frac{1}{1 + A\left(\frac{\sigma_0}{f_c}\right)^{b-1}}, \left(\frac{\sigma_0}{f_c} \le 2\right) \tag{4}$$

$$\frac{K_s}{K_e} = \frac{1}{1 + 2^{b-1}Ab - 2^b(b - 1)A\left(\frac{\sigma_0}{f_c}\right)^{-1}}, \left(\frac{\sigma_0}{f_c} > 2\right) \tag{5}$$

$$\frac{G_s}{G_e} = \frac{1}{1 + C\left(\frac{\tau_0}{f_c}\right)^{d-1}} \tag{6}$$

Where, K_e = initial bulk modulus.

To get a constitutive relation, a tangential modulus is deduced

$$E_t = \frac{9K_tG_t}{3K_t + G_t}; \nu_t = \frac{3K_t - 2G_t}{6K_t + 2G_t}$$

Where, K_t = tangent bulk modulus, G_t = shear modulus. The formula is expressed as

$$\frac{K_t}{K_e} = \frac{1}{1 + bA\left(\frac{\sigma_0}{f_c}\right)^{b-1}}, \left(\frac{\sigma_0}{f_c} \le 2\right) \tag{7}$$

$$\frac{K_t}{K_e} = \frac{1}{1 + 2^{b-1}Ab}, \left(\frac{\sigma_0}{f_c} > 2\right) \tag{8}$$

$$\frac{G_t}{G_e} = \frac{1}{1 + dC\left(\frac{\tau_0}{f_c}\right)^{d-1}} \tag{9}$$

Where,

A, C, a, b, c and d are material parameters (Equations 4-9).

Parameters of formulae from four to nine can be acquired from Equations 4-9.While considering the particularity of concrete in concrete-filled steel tubes, μ_c is expressed as

$$\mu_c = \begin{cases} 0.173 & \sigma_3 \le 0.4\sigma_0 \\ 0.173 + 0.7036\left(\dfrac{\sigma_3}{\sigma_0} - 0.4\right)^{1.5} & \sigma_3 > 0.4\sigma_0 \end{cases}$$

$$(10)$$

Where

σ_3 = longitudinal stress

Assuming an equality of the longitudinal modulus of elasticity and transverse modulus of elasticity

$$E_c = E_s, G_c = \frac{E_c}{2(1 + \mu_c)} \qquad (11)$$

Where,

E_c = transverse modulus of elasticity;

G_c = shear modulus.

In conclusion, the formulae are given as

$$\varepsilon_{ij} = \frac{\sigma_{ij} + \sigma_{id}\delta_{ij}}{2G_s} - \frac{3\nu_s}{E_s}\left(\sigma_0 + \sigma_{id}\right)\delta_{ij}$$

$$\left(\varepsilon_{33}, \varepsilon_{13}, \varepsilon_{23}\right) \qquad (12)$$

$$\varepsilon_{ij} = \frac{\sigma_{ij}}{2G_c} - \frac{3\upsilon}{E_s}\sigma_0\delta_{ij} \qquad \left(\varepsilon_{11}, \varepsilon_{12}, \varepsilon_{22}\right) \qquad (13)$$

When the concrete is crazing,

$$\delta\varepsilon_0 = \frac{1}{3}\left(\delta\varepsilon_1 + \delta\varepsilon_2 + \delta\varepsilon_3\right) \qquad (14)$$

Where

$\delta\varepsilon_1, \delta\varepsilon_2, \delta\varepsilon_3$ = the strain of principal stress direction

$$\delta\varepsilon_3 = \frac{3\delta\varepsilon_0}{1 + \gamma_{23} + \gamma_{13}}, \delta\varepsilon_2 = \gamma_{23}\delta\varepsilon_3, \delta\varepsilon_1 = \gamma_{13}\delta\varepsilon_3$$

$$(15)$$

Assume there is a certain functional relation between $\delta\varepsilon_0, \sigma_0$ and $\delta\tau_0$

$$\delta\varepsilon_0 = \left[-45.8 - 71.4\left(\frac{\sigma_0}{f_c}\right)\right]\delta\tau_0^2 \Big/ f_c^2 \qquad (16)$$

Where σ_0 and $\tau_0 =$ octahedral normal stress and octahedral shear stress

$\delta\tau_0 = \tau_0 - \tau_{OUFP}$

Parameters of formulae obtained from [19].

3   Experimental study

To understand the basis of the numerical modeling method and assess the accuracy of the numerical simulations, it is necessary to provide a description of the physical tests and the main experimental observations. All tests were performed in a TYS-500 long column testing machine at College of Civil Engineering and Architecture of Central South University. For each test specimens, with the test machine, and software, it was possible to automatically capture axial load and axial displacement . Axial lateral strain through DH3818 static strain gauge automates data acquisition and storage by a computer and the data acquisition frequency is 2 times per second. The test set-up is shown in Fig.1. While minute eccentricities might occur, every effort has been made to reduce the effect of the eccentric loading to ensure that the columns were concentrically and uniformly loaded [20].

3.1 Compressive stub column tests

In total, 2 concrete-filled steel tube column specimens were tested at Central South University in order to investigate: (1) the axial compressive behavior of short concrete-filled steel tube columns with different concrete grades. Of the 2 tests, two specimens were compositely loaded with the concrete core and hollow section steel tube to investigate the effect of concrete strength on the axial compressive behavior of short composite columns. The numerical modelling method presented will mainly be focusing on the axial compressive behavior of short concrete-filled composite columns compositely loaded and will not take into account the concrete shrinkage effect. The measured unconfined compressive cube strengths for concrete grades see Table 1, respectively. Table 2 shows the measured dimensions and material properties of the circular hollow sections. In order to study the convenient, the G106 and G132 specimens loaded will be modeled in this paper.
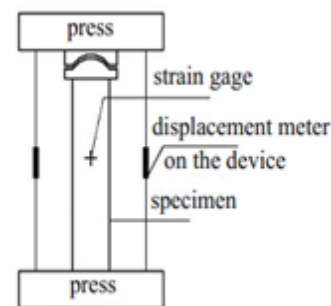

Figure 1. Test set up.

3.2 Experimental analysis

Fig. 2 presents the axial compressive load versus the average axial strain relationship. Based on the experimental studies of 2 short steel tubular columns filled with super high strength concrete used stone-chip , it is found that within the factor

scope of these tests, both the confinement index and the concrete strength of the specimens have great influence on their features of specimen subjected to the axial load. Experiment results show that the load & average strain curves of the specimens might be divided into four stages: elastic deformation process, elastic-plastic deformation process, the descent process and the recovery process of its carrying capacity, and also that specimens with the lower confinement index exhibit a rapid softening process in the post-peak region with a towering peak and a shorter incremental portion plus the weak recovery in the four stage, while specimens with the higher confinement index exhibit a gradual softening process in the post-peak region with a chubby curve and a longer incremental portion plus the strong momentum of recovery in the forth The experimental phenomena indicate that all specimens are typical of the higher residual load capacity and excellent ductility.
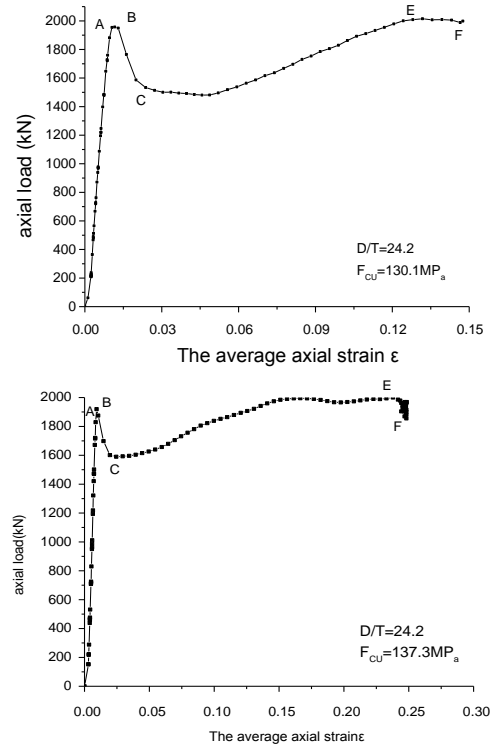

Figure 2. Load-steel tube average strain curve.

Table 1. Mix of extra-high strength concrete mixed with stone-chip.

| Mix type | Mix | | | | | | | Water-binder ratio | Cement content | f_{cu} |
	Cement	Silica fume	Metakaolin	Fly ash	Rock ballast	Macadam	Water reducer		$kg \cdot m^{-3}$	MP_a
A3	1	0,167	0,167:	0,333	2,028	3,056	0,0694	0,22	350	137,3
A5	1	0,175	0,175:	0,338	1,75	2,575	0,0625	0,22	380	130,1

Where, f_{cu} = compressive strength

Table 2. Parameters of specimens

Specimen number	$D \times t$ mm	D/t	L mm	L/D	f_y MP_a	Mix type	f_{cu} MP_a	θ
G106	121,0×5.0	24,2	370	3,1	295	A3	137,3	0,57796
G132	121,0×5,0	24,2	370	3,1	295	A5	130,1	0,60994

Where , D= outer diameter of steel tube, t= thickness of the steel pipe, f_y =yield strength of steel tube
θ= generalized ferrule indicators, L= length of steel tube.

4   Description of the numerical modeling method

There is no doubt that full-scale physical testing provides a better insight into the understanding of the behavior of the structural members; however, physical testing is expensive and time consuming, and it is also very difficult to conduct extensive parametric studies by experiments, thus encouraging

the use and development of numerical modeling in engineering researches. Many numerical models have been proposed to predict the behavior of concrete-filled steel tube columns following the increasing use of composite columns in modern buildings [21-25].

As observed from the experiments, the failure modes of short concrete-filled steel tubular columns under axial compressive loads are characterized by yielding

_____

of the hollow sections and concrete crushing, which differ from slender concrete-filled tubular columns under axial compressions whose failure mode is generally global buckling. This suggests that the axial compressive behavior of short concrete-filled column depends on the material properties of the constituent members and their composite action.

4.1 Finite element (FE) model

The FE model developed through the ABAQUS/Standard solver will be used to simulate the concrete-filled circular steel stub columns under axial compression.

Fig.3 shows a typical FE model in which three-dimensional 8-node solid elements (C3D8) were adopted for both the elliptical steel hollow section and the confined concrete core. Considering the effects of other factors on the predicted structural behavior in numerical models, such as the stub column dimensions, the appropriate mesh size would be 5–10 mm for the steel hollow section and 10–20 mm for the concrete, i.e., the concrete element size is about twice the element size of the steel hollow section.

From Fig.1, it can be seen that two loading plates were used at the column ends; therefore, two rigid plates were modeled to simulate these plates, as shown in Fig.3. Both in the tests and FE modeling, the load is applied to the column through the top loading plate. In the test, a direct contact existed between the end plates and the end surfaces of the short column; therefore a contact function available in the ABAQUS/Standard solver was used to simulate the interaction between the rigid plate and the column end surface.

In the FE model, the lower rigid plate contacting the bottom of the column was fixed in all six directions by the reference node, and the upper rigid plate to the top of the column was fixed in five directions allowing only movement in the column axis at the reference node. The column end restraints adopted in the FE model were identical to the testing procedures; no other translations and rotations were observed in tests at both loading plates.

4.2 Comparison between the numerical and experimental results

The accuracy of the finite element model developed through the ABAQUS/Standard solver combined with the proposed stress–strain model for the confined concrete was verified by comparing the numerical results with the experimental results. The maximum compressive load, load versus column end-shortening and the column deformed shape were investigated.

Table 3 shows a comparison between the maximum axial compressive loads (P_{Test}) obtained from the experiments and the maximum axial compressive loads (P_{FE}) predicted by the finite element models: very good agreements have been obtained. The maximum difference observed between the experimental and numerical results is 5%.

5 Conclusion

According to the continuous mechanics, the relationship of mathematical description to the concrete deformation behaviors was proposed in this paper. Meanwhile, this paper provides the simulation in developing a numerical model through the ABAQUS/Standard solver to investigate the axial compressive behavior of ultra- strength concrete-filled circular steel stub columns. The feasibility and accuracy of the numerical method and the proposed stress–strain model were verified by comparing the predicted results with the experimental observations, and the following conclusions are made:

The FE numerical method developed via the ABAQUS/ Standard solver could be used to predict the main structural behavior of ultra- strength concrete-filled steel tube columns under axial compressive loads.

One of the difficulties in verifying the potential of the material model for the one-dimensional bond interface element developed in this study is the lack of available experimental data.. Further studies are needed to collect data on the key modeling parameters.
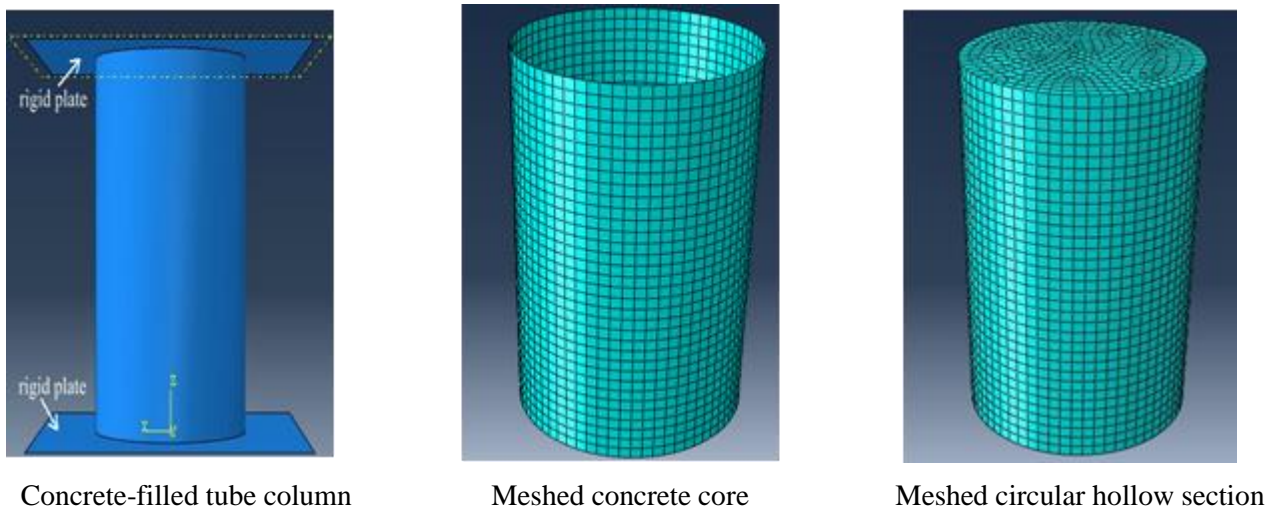
Concrete-filled tube column   Meshed concrete core   Meshed circular hollow section

Figure 3. Typical FE model adopted in numerical modelling.

Table 3. Comparison of maximum loads from experiments and numerical prediction

Specimen number	Maximum load by test, P_{Test}	Maximum load by model, P_{FE}	P_{Test}/P_{FE}
	kN	kN	
G106	1919,823	1863,906	1,03
G132	1957,047	1863,854	1,05

Acknowledgements

References

[1] Seanz L. P. :*Discussion of a paper by Desayi and Krishnan S, equation for the stress-stain curve of concrete*, Journal of ACI, 61 (1964) 9, 381-393.

[2] Gopalaratnam V S , Surendra P S. : *Softening response of pain concrete in direct tension*, Journal of ACI, 82(1985) , 3, 310-323.

[3] Morino S. : *Recent developments in hybrid structures in Japan-research, design and construction*, Engineering Structures, 20(1998), 4–6,336–346.

[4] Shanmugam NE, Lakshmi B. : *State of the art report on steel–concrete composite columns*, Journal of Constructional Steel Research, 57(2001),1041–80.

[5] Johansson M., Gylltoft K.: *Mechanical behavior of circular steel-concrete composite stub columns*, Journal of Engineering Mechanics, 128(2002) 8,1073-1081.

[6] Hajime O., Masahiro O.: *Self-compacting concrete*, Journal of Advanced Concrete Technology, 1 (2003),1,5-151.

[7] Ehab E., Ben Y., Dennis L.: *Behavior of normal and high strength concrete-filled compact steel tube circular stub columns*, Journal of Constructional Steel Research, 7 (2006) 62, 706-715.

[8] Dai X., Lam D.: *Numerical modelling of the axial compressive behaviour of short concrete-filled elliptical steel columns*, Journal of Constructional Steel Research, 66 (2010), 931–942.

[9] Chang-Jian Z., Yi Y. and Tian-Ling R.: *Finite element analysis of lateral field excited thickness shear mode film bulk acoustic resonator*, The International Journal for Computation and Mathematics, 31 (2012) 6, 1892-1900.

[10] Kam Y., Loo1 M., Foster S. J. and Smith S. T., Asce M.: *FE Modeling of CFRP-Repaired RC Beams Subjected to Fatigue Loading*, Journal of composites for construction, 16 (2012), 572-580.

_____

[11] Anas R., Noureddine A., Mohamed B: *Two-level Finite Volume Methods and some a priori estimates For Steady Navier-Stokes Equations*, The International Journal for Computation and Mathematics, 23(2014) 2 ,104-115.

[12] Van G. A, Taerwe L.: *Analytical formulation of the complete stress-strain curve for high strength concrete*, Materials and Structures, 29 (1996) 11,529-533.

[13] Kotsovos M. D., Newman J. B.: *A mathematical description of the deformational behavior of concrete under complex loading*, Mag. Res. 107 (1979), 77-90.

[14] Qian X., Li Z. : *The relationships between stress and strain for high-performance concrete with metakaolin*, Cement and Concrete Research, 31 (2001) 11, 1607-1611.

[15] Johansson Mathias, Gylltoft Kent. : *Mechanical behavior of circular steel-concrete composite stub columns*, Journal of Engineering Mechanics, 128 (2002) 8, 1073-1081.

[16] Huang C.S., Yeh Y.K., Liu G.Y. at el. : *Axial load behavior of stiffened concrete- filled steel columns*, Journal of Structural Engineering, 128 (2002) 9, 1222-1230.

[17] Giakoumelis G., Lam D.: *Axial capacity of circular concrete-filled tube columns*, Journal of Constructional Steel Research, 60 (2004) 7, 1049-1068.

[18] Chen H., Zhong S. and Zhang S.: *Three dimensional stress-strain relation of concrete in concrete-filled steel tubes*, Journal of Harbin University of C. E. & Architecture, 33 (2000) 3, 13-16.

[19] Chen G., Xu Z., Yang Z., Tian Z.: *Experimental study on behavior of short steel tubular columns filled with ultra-high strength concrete mixed with stone-chip subjected to axial load*, Journal of building structures, 32 (2011) 3, 82-89.

[20] Fam A. Z., Rizkalla S. H.: *Confinement model for axially loaded concrete confined by circular FRP tubes*, Aci Structure Journal, 98 (2001) 4, 451-461.

[21] Omar C., Mohsen S.: *Performance of fiber-reinforced polymer - wrapped reinforced concrete column under combined axial-flexural loading*, Aci Structure Journal, 97 (2001) 4, 659-668.

[22] Hu H., Huang C. S., Chen Z. L.: *Finite element analysis of CFT columns subjected to an axial compressive force and bending moment in combination*, Journal of Constructional Research, 61 (2005) 12,1692-1712.

[23] Luccioni, B., Ruano, G., Isla, F., Zerbino, R., Giaccio, G.: *A simple approach to model SFRC*, Construction and Building Materials, 37 (2012), 111–124

[24] Alih, S., Khelil, A.: *Behavior of inoxydable steel and their performance as reinforcement bars in concrete beam: Experimental and nonlinear finite element analysis*, Construction and Building Materials, 37 (2012), 481–492.